A method to estimate the reflection and tunneling of ocean waves at a submarine canyon*

Jim Thomson
WHOI-MIT Joint Program in Oceanography, Woods Hole, Massachusetts, USA

Steve Elgar
Woods Hole Oceanographic Institution, Woods Hole, Massachusetts, USA

T.H.C. Herbers
Naval Postgraduate School, Monterey, California, USA

In contrast to methods used to estimate the amount of reflection from impermeable structures [*Dickson et al.,* 1995], estimation of the reflection of a canyon must also account for transmission. Here, inverse techniques [*Coleman and Li,* 1996] are used to determine the reflection (R_s, R_n) and transmission (T_s, T_n) coefficients, as well as the incident directional spectra (D_s, D_n) and reflected phases (ψ_s, ψ_n) of the wave fields on the south (s) and north (n) sides of the canyon that are most consistent with observations of pressure and velocity.

The random wave fields on the north (n) and south (s) sides of the canyon consist of incident, reflected, and transmitted (from the other side of the canyon) waves such that the surface elevations η_s and η_n can be written as integrals over wave components at each frequency and direction, given by Eqs. 4 and 5, and repeated here for convenience:

$$\eta_\mathrm{s} = \int_\omega \int_{\theta=-\frac{\pi}{2}}^{\frac{\pi}{2}} d_\mathrm{s} \left(\mathrm{e}^{i(mx+ly-\omega t)} + R_\mathrm{s} \mathrm{e}^{i(mx-ly-\omega t+\psi_\mathrm{s})} \right) + d_\mathrm{n} \left(T_\mathrm{n} \mathrm{e}^{i(mx-ly-\omega t)} \right), \tag{A1}$$

$$\eta_\mathrm{n} = \int_\omega \int_{\theta=-\frac{\pi}{2}}^{\frac{\pi}{2}} d_\mathrm{n} \left(\mathrm{e}^{i(mx-ly-\omega t)} + R_\mathrm{n} \mathrm{e}^{i(mx+ly-\omega t+\psi_\mathrm{n})} \right) + d_\mathrm{s} \left(T_\mathrm{s} \mathrm{e}^{i(mx+ly-\omega t)} \right), \tag{A2}$$

where d_s and d_n are the complex-valued differential amplitudes of the incident wave components at radian frequency ω and direction θ relative to the cross-canyon coordinate y. The variables R_s, R_n and T_s, T_n are reflection and transmission coefficients, x is the along-canyon coordinate, and t is time. The along-canyon (x) and cross-canyon (y) components of the wavenumber vector are $m = k \sin\theta$ and $l = k \cos\theta$, respectively. In this two-quadrant ($-\frac{\pi}{2} < \theta < \frac{\pi}{2}$) system, the direction of y propagation is given explicitly by the sign of the exponent in $\mathrm{e}^{\pm ly}$ because l is always positive.

Assuming specular reflection, the reflected wave fields have amplitudes $R_\mathrm{s} d_\mathrm{s}$ and $R_\mathrm{n} d_\mathrm{n}$ that propagate away from the canyon (i.e., $\mathrm{e}^{\mp ly}$) with phase shifts ψ_s and ψ_n relative to the incident wave field. Conserving

*This is auxiliary material to *Geophysical Research Letters*, **32**, DOI: 10.1029/2005GL022834, and is available online at ftp://agu.org/apend/gl/2005GL022834/. Hard copies are available by e-mailing jthomson@whoi.edu or elgar@whoi.edu.

energy, the remaining (i.e., nonreflected) portion of the wave field is transmitted across the canyon with amplitudes $T_\mathrm{s}d_\mathrm{s}$ and $T_\mathrm{n}d_\mathrm{n}$.

The cross-canyon velocity v, along-canyon velocity u, and pressure p fields induced by surface waves (Eqs. A1 and A2) can be determined from a linear, hydrostatic momentum balance (appropriate for infragravity waves in 20-m water depth) given by

$$\frac{\partial v}{\partial t} = -g\frac{\partial \eta}{\partial y}, \quad \frac{\partial u}{\partial t} = -g\frac{\partial \eta}{\partial x}, \quad p = \rho g \eta, \tag{A3}$$

where g is gravitational acceleration and ρ is density.

Substituting η_s and η_n into the momentum balance (Eq. A3), using the Fourier transformed result, and applying the identities $2\mathbf{i}\sin(\mathbf{i}\alpha) = \mathrm{e}^{-\alpha} - \mathrm{e}^{\alpha}$ and $2\cos(\mathbf{i}\alpha) = \mathrm{e}^{\alpha} + \mathrm{e}^{-\alpha}$ yields the following expressions for the frequency cross-spectra of the colocated pressure and velocity time series south (s) of the canyon

$$\langle p_\mathrm{s}(\omega)\cdot u_\mathrm{s}^\star(\omega)\rangle = \rho g\kappa \int_\theta \sin\theta \left[D_\mathrm{n}T_\mathrm{n}^2 + D_\mathrm{s}\left(1 + R_\mathrm{s}^2 + 2R_\mathrm{s}\cos\psi_\mathrm{s}\right)\right] d\theta, \tag{A4}$$

$$\langle p_\mathrm{s}(\omega)\cdot v_\mathrm{s}^\star(\omega)\rangle = \rho g\kappa \int_\theta \cos\theta \left[-D_\mathrm{n}T_\mathrm{n}^2 + D_\mathrm{s}\left(1 - R_\mathrm{s}^2 + \mathbf{i}2R_\mathrm{s}\sin\psi_\mathrm{s}\right)\right] d\theta, \tag{A5}$$

$$\langle u_\mathrm{s}(\omega)\cdot v_\mathrm{s}^\star(\omega)\rangle = \kappa^2 \int_\theta \sin\theta\cos\theta \left[-D_\mathrm{n}T_\mathrm{n}^2 + D_\mathrm{s}\left(1 - R_\mathrm{s}^2 + \mathbf{i}2R_\mathrm{s}\sin\psi_\mathrm{s}\right)\right] d\theta, \tag{A6}$$

where $\kappa = \frac{gk}{\omega}$, $\star$ is the complex conjugate, and $\langle\rangle$ is the expected value. Similarly, the auto-spectra are

$$\langle p_\mathrm{s}(\omega)\cdot p_\mathrm{s}^\star(\omega)\rangle = (\rho g)^2 \int_\theta \left[D_\mathrm{n}T_\mathrm{n}^2 + D_\mathrm{s}\left(1 + R_\mathrm{s}^2 + 2R_\mathrm{s}\cos\psi_\mathrm{s}\right)\right] d\theta, \tag{A7}$$

$$\langle u_\mathrm{s}(\omega)\cdot u_\mathrm{s}^\star(\omega)\rangle = \kappa^2 \int_\theta \sin^2\theta \left[D_\mathrm{n}T_\mathrm{n}^2 + D_\mathrm{s}\left(1 + R_\mathrm{s}^2 + 2R_\mathrm{s}\cos\psi_\mathrm{s}\right)\right] d\theta, \tag{A8}$$

$$\langle v_\mathrm{s}(\omega)\cdot v_\mathrm{s}^\star(\omega)\rangle = \kappa^2 \int_\theta \cos^2\theta \left[D_\mathrm{n}T_\mathrm{n}^2 + D_\mathrm{s}\left(1 + R_\mathrm{s}^2 - 2R_\mathrm{s}\sin\psi_\mathrm{s}\right)\right] d\theta, \tag{A9}$$

The incident wave directional spectra D_s and D_n are defined as

$$D_s(\omega,\theta) = \frac{\langle d_s \cdot d_s^\star\rangle}{d\omega d\theta}, \tag{A10}$$

$$D_n(\omega,\theta) = \frac{\langle d_n \cdot d_n^\star\rangle}{d\omega d\theta}. \tag{A11}$$

The incident waves fields on the north and south sides of the canyon are independent of each other, and thus $\langle d_s \cdot d_n^\star\rangle = \langle d_n \cdot d_s^\star\rangle = 0$.

Expressions for cross- and auto-spectra at the north side of the canyon are obtained by exchanging all subscripts (s↔n) in the expressions above (Eqs. A4-A9) and changing the sign of the integrand in Eqs. A5 and A6.

The real-valued terms describe the progressive wave field, and the imaginary ($\mathbf{i}$) terms (i.e., the quadrature in the cross-spectra $\langle p\cdot v^\star\rangle$ and $\langle u\cdot v^\star\rangle$) describe the partial standing wave patterns owing to

sums of incident and reflected waves. In practice, the expressions for cross- and auto-spectra apply only to observations near the canyon walls, because over large distances (i.e., many wavelengths) standing wave patterns are obscured within a finite-width frequency band.

For computational efficiency, the incident directional spectra (Eqs. A10 and A11) at each frequency band are modeled as [*Donelan et al.,* 1985]

$$D_{\rm s}(\theta) = M_{\rm s} \cos^{2S_{\rm s}} \left(\frac{\theta - \Theta_{\rm s}}{2} \right), \tag{A12}$$

$$D_{\rm n}(\theta) = M_{\rm n} \cos^{2S_{\rm n}} \left(\frac{\theta - \Theta_{\rm n}}{2} \right), \tag{A13}$$

where $\Theta_{\rm s}$ and $\Theta_{\rm n}$ are the centroidal directions, $S_{\rm s}$ and $S_{\rm n}$ describe the spread in direction about the centroid, and $M_{\rm s}$ and $M_{\rm n}$ are the spectral peak values. The results are insensitive to the specific unimodal shape used for the incident directional spectra. The centroidal directions $\Theta_{\rm s}$ and $\Theta_{\rm n}$ were used to separate the data sets (at each frequency band) into normally ($|\Theta| < 20°$) and obliquely ($|\Theta| > 30°$) incident waves. Assuming directionally narrow spectra, the reflection ($R_{\rm s}, R_{\rm n}$) and transmission ($T_{\rm s}, T_{\rm n}$) coefficients are assumed to be independent of direction at each frequency. The spreading parameters ($S_{\rm s}$, $S_{\rm n}$) were used to weight individual estimates of R^2 before averaging over the collection of data runs (e.g., the symbols in Figure 2).

The phase shifts $\psi_{\rm s}$ and $\psi_{\rm n}$ of the reflected waves relative to the incident waves were allowed to vary over each directional spectrum by assuming

$$\psi_{\rm s}(\theta) = 2\Delta y_{\rm s} k \cos\theta, \tag{A14}$$

$$\psi_{\rm n}(\theta) = 2\Delta y_{\rm n} k \cos\theta, \tag{A15}$$

where $\Delta y_{\rm s}$ and $\Delta y_{\rm n}$ are the (unknown) distances between the reflector and the instrument locations (i.e., ψ is the phase change associated with propagating toward and back from the reflector). The resulting inverse estimates of $\Delta y_{\rm s}$ and $\Delta y_{\rm n}$ are consistent with the measured distances (Figure A1). The small deviations from theory may be caused by incorrectly assuming all the reflection takes place at a single location.

Assuming energy is conserved (i.e., $R_{\rm s}^2 + T_{\rm s}^2 = 1$, $R_{\rm n}^2 + T_{\rm n}^2 = 1$), the inverse method finds the north (n) and south (s) values of Θ, S, M, R, and Δy that are most consistent with the cross- and auto-spectra of the observed time series by minimizing a normalized root-mean-square error [*Dickson et al.,* 1995]

$$\epsilon = \sqrt{\frac{\sum (obs - derived) \cdot (obs - derived)^\star}{\sum (obs)(obs)^\star}}, \tag{A16}$$

where $\sum$ is the sum over the six spectral values from the south side (Eqs. A4-A9) and the six spectral values from the north side. Applying recent improvements to Newton's method [*Coleman and Li,* 1996],

the inverse algorithm begins with an initial guess for each unknown, and solves a locally linearized version of the equations for the cross- and auto-spectra to find the small change in each unknown that produces the greatest reduction in ϵ (i.e., the method iterates down-slope in ϵ until the minimum is found). Initial guesses for Θ, S, and M are provided by estimates of directional moments of the wave field based on the measured pressure and velocities [*Kuik et al.,* 1988], and the initial guesses for R are based on long-wave theory [*Kirby and Dalrymple,* 1983]. The results are not sensitive to the initial values, and the same inverse solutions are obtained with random initial guesses (although computational time is increased).

The residual errors (Eq. A16) approximately follow the expected χ^2 distribution of fluctuations in spectral estimates from finite length data records [*Wunsch,* 1996]. The percent of observed variance captured by the inverse method (defined as $100 \times [1 - \epsilon^2]$) is 90% when averaged over all infragravity frequency bands for all 50 data sets.

References

Coleman, T., and Y. Li (1996), An interior, trust region approach for nonlinear minimization subject to bounds, *SIAM J. Optimization*, *6*, 418-445.

Dickson, W., T.H.C. Herbers, and E. Thornton (1995), Wave reflection from breakwater, *J. of Water., Port, Coast., Ocean Eng.* **121**, 262-268.

Donelan, M., J. Hamilton, and W. Hui (1985), Directional spectra of wind-generated waves, *Phil. Trans. Roy. Soc. Lon.* **A315**, 509-562.

Kuik, A., G. Van Vledder, and L. Holthuijsen (1988), A method for the routine analysis of pitch-and-roll buoy wave data, *J. Phys. Oceanog.* **18**, 1020-1034.

Wunsch, C. (1996), *The Ocean Circulation Inverse Problem* (Cambridge University Press, Cambridge).

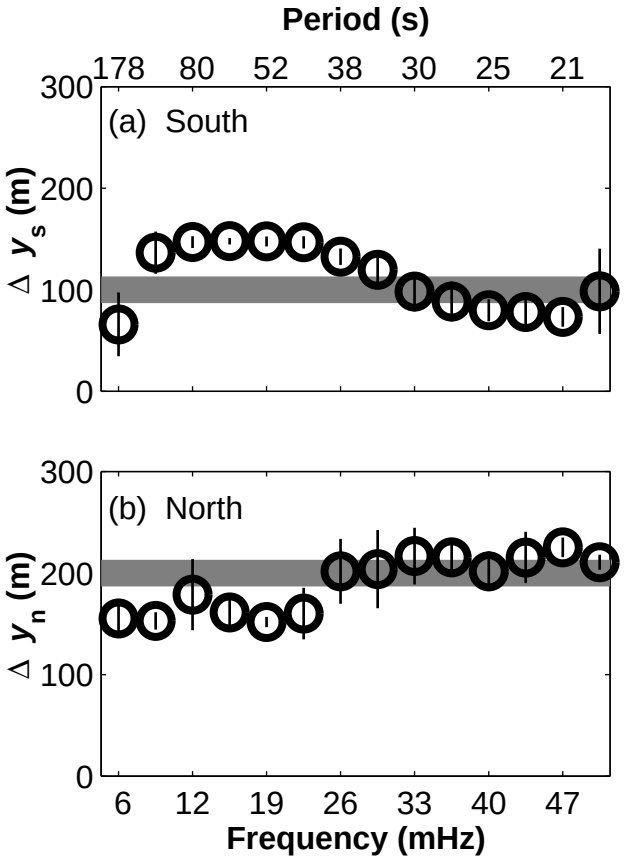

Figure A1: Distance (m) between the reflector and the instrument location versus frequency (mHz) and period (s) at the (a) south and (b) north sides of the canyon. Symbols are estimates from the nonlinear inverse method and solid lines are the measured distances from the steepest portion of each canyon slope to the instrument site at that side. Instrument locations were determined within $\pm$ 10 m (the width of the solid lines) with differential GPS. The theory assumes that waves propagate from the instrument site to a vertical-canyon-wall reflector along a line of constant y and back, neglecting possible phase shifts at the sloped walls. Vertical lines are $\pm$ one standard deviation of the estimates.